available at www.sciencedirect.com

ScienceDirect

journal homepage: www.elsevier.com/locate/agrformet

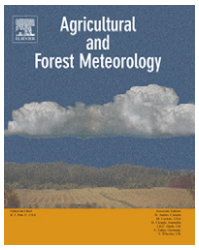

Surface energy-balance closure over rangeland grass using the eddy covariance method and surface renewal analysis

F. Castellví [a,*], R.L. Snyder [b], D.D. Baldocchi [c]

[a] University of Lleida, Spain
[b] University of California, Department of Land, Air and Water Res, Davis, CA, USA
[c] University of California, Department of Environmental Science, Policy & Management, Berkeley, CA, USA

ARTICLE INFO

Article history:
Received 7 September 2007
Received in revised form
13 February 2008
Accepted 29 February 2008

Keywords:
Sensible heat flux
Latent heat flux
Carbon dioxide flux
Surface energy-balance
Surface renewal
Bowen ratio

ABSTRACT

The performance of surface renewal (SR) analysis for estimating sensible heat (H), latent heat (L_wE) and carbon dioxide (L_pF_p) flux, and the closure of the surface energy-balance equation were analyzed in an experiment at a rangeland grass site in the foothills of the Sierra Nevada Mountains (Ione, CA, USA). Both the L_wE and H fluxes in late fall, winter, and early spring (the wet period) were relevant in the energy-balance, but from early spring to fall (dry period), most of the available net surface-energy contributed to sensible heat flux. The site is influenced by regional advection and some degree of dissimilarity between temperature and the other two scalars was observed. To our knowledge, this is the first paper evaluating the capability of SR analysis to (1) close the energy-balance on a long-term experiment and (2) estimate carbon dioxide flux. The SR analysis performance was evaluated in terms of the correlation with fluxes from the eddy covariance (EC) method and its capability to close the surface energy-balance. Regardless of the weather conditions, the EC closure underestimated the available energy by about 10%, but the performance was slightly better during dry rather than humid conditions. In contrast, the SR closure was always good and did not favor wetness conditions. Despite the lack of similarity, the energy partitioning provided by SR analysis was reliable for all three scalars. SR analysis provided reliable Bowen ratio estimates. Under stable atmospheric conditions fluxes were too small to evaluate either method.

1. Introduction

Energy budgets are typically evaluated within a volume that includes the vegetation above a surface. Provided that homogeneity and stationary conditions are met, time averaged energy fluxes are vertical and the sum of sensible heat, H, latent heat, L_wE, and carbon dioxide, L_pF_p, flux at the top of the volume equals all other surface energy sinks and sources

$$H + L_wE + L_pF_p = R_n - G - S \quad (1)$$

where L_w is the latent heat of vaporization, E is the flux of water vapor, L_p is the thermal conversion factor for fixation of carbon dioxide, F_p is the flux of carbon dioxide, R_n is the net radiation, G is the soil heat flux and S is the total rate of energy storage (air and biomass below the measurement of R_n) within the volume per unit area. Typically, L_pF_p and S are small and neglected for short vegetation (Brutsaert, 1988). Hence, Eq. (1) simplifies to

$$H + L_wE = R_n - G \quad (2)$$

* *Corresponding author at*: Dpt. Medi Ambient i Cienciès del Sòl, E.T.S.E.A. C. Rovira Roure, 191, Lleida 25198, Spain. Tel.: +34 973 702620; fax: +34 973 702613.
E-mail address: f-Castellvi@macs.udl.es (F. Castellví).
0168-1923/$ – see front matter
doi:10.1016/j.agrformet.2008.02.012

Although the homogeneous surface area needed to measure a representative value for R_n and G is small, the "foot prints" for H and L_wE are much larger (especially under stable conditions). If the footprints fall within the measurement surface area, then the available net surface energy (i.e., the right-hand side of Eq. (2)) should equal the sum of H and L_wE. At flat and extensive homogeneous locations, an imbalance in Eq. (2) is an indicator of the instrument inaccuracy or shortcomings and/or a lack of understanding of all transport processes and assumptions made in turbulent flux determinations (Baldocchi, 2008; Oncley et al., 2007; Kohsiek et al., 2007; Wilson et al., 2002). According to Twine et al. (2000), measurements over near ideal sites of 0.25–1.0 m tall grazed pasture and rangeland grass showed that half-hourly eddy covariance, EC, H and L_wE data during periods with $R_n - G > 0$, the $H + L_wE$ averages were within 77–87% of measured $R_n - G$, and the probable error was estimated to be within 6%. While the Twine et al. (2000) paper showed that energy-balance closure is a problem in near ideal conditions, the underestimation of the actual $H + L_wE$ is a historical problem, which has long-term implications for water management assessment in agriculture, carbon sequestration, and climate model validations and calibrations (Oncley et al., 2007; Baldocchi et al., 2004).

Based on similarity in mechanisms of scalar turbulent transport, some authors assume that the unexplained portion of each turbulent energy flux is the same regardless of the scalar (Laubach and Teichmann, 1999; Twine et al., 2000). Forcing closure using the Bowen ratio, was suggested as a turbulent flux correction (Twine et al., 2000). Other authors attribute the lack of closure to instrument shortcomings and imply that the EC method is more accurate for estimating H (Kristensen et al., 1997). Therefore, by invoking *similarity*, the unexplained portion of L_wE and L_pF_p should be similar. We note that now *similarity* involves the same mechanisms of turbulent transport and that measurement of L_wE and L_pF_p may share common instrumentation. Other studies emphasize the need to consider all the terms involved in the energy-balance (Meyers and Hollinger, 2004; Oncley et al., 2007). While the preferred method for measuring turbulent fluxes is the EC method, the lack of closure is unresolved and a full guidance (manual) on experimental set up and raw data processing for eddy covariance systems is still unavailable (Mauder et al., 2007). In addition, the EC method is not always affordable, and the high cost may limit the number of desired measurements in a given study or the number of experiments conducted. Surface renewal, SR, theory (Higbie, 1935) in conjunction with the analysis of the observed ramp-like patterns in the scalar traces (Paw U et al., 1995) provides an advantageous method for estimating the surface flux density of a scalar (Drexler et al., 2004). SR analysis is a simple, transilient theory that is Lagrangian in nature, which is based on the scalar conservation equation. It has the advantages that (1) the measurement of the scalar trace is the only input required and (2) it operates in either the roughness or inertial sub-layers. Thus, SR analysis minimizes typical problems related to fetch requirements, levelling, shadowing, orientation, relative instrument-separation, and rotation, which introduce potential uncertainties in the EC and other methods based on profiles. A detailed review of SR analysis is given in Paw U et al. (2005) and the performance of new SR analysis-based equations over a variety of canopies are shown in Castellvi (2004), Castellvi and Martinez-Cob (2005) and Castellvi et al. (2006a,b). There are few papers evaluating the performance on SR analysis on L_wE because (1) air temperature is easier and less expensive to measure, (2) one can evaluate the performance of the sensible heat flux estimates by comparison with the EC method (a reference), and (3) the latent heat flux can be estimated as a residual of Eq. (2) (Snyder et al., 1996; Spano et al., 1997, 2000; Zapata and Martinez-Cob, 2001; Anderson et al., 2003). This implies that the error in L_wE is the sum of errors in R_n, G and H, and therefore, accurate H estimates are required. To our knowledge, there are two SR papers evaluating latent heat flux from humidity traces (Katul et al., 1996; Castellvi et al., 2006b) and only a short communication on CO_2 flux over a tall forest (Spano et al., 2002) using the SR method described in Snyder et al. (1996).

This paper evaluates the performance of the SR analysis of data collected over rangeland grass based on the equation previously described in Castellvi (2004) for estimating H, L_wE and L_pF_p. In addition to high frequency scalar measurements, the mean wind speed at a reference level is required as an input. A cup anemometer, however, is a low-budget and robust instrument. In some earlier SR studies (Snyder et al., 1996; Zapata and Martinez-Cob, 2001; Castellvi et al., 2002), above canopy mean wind speed was not used, but the SR method did require calibration against EC measurements. Calibration mainly varies with changing canopy characteristics and atmospheric surface layer stability conditions. Originally, the scalar data were measured and stored at high frequency in computers (Chen et al., 1997a), which made SR analysis impractical for long-term field applications (Chen et al., 1997b). Later, however, Paw U et al. (2005) described a method to store statistical moments in a data logger for later computer analysis, which simplified the procedures to collect field data.

2. Theory

Consider an air parcel, with some scalar concentration, traveling at a given height above the surface. SR analysis assumes that at some instant the parcel suddenly moves down to the surface and remains connected with the sources (sinks) for a period of time during which it is horizontally traveling along the sources. By continuity, the parcel ejects upwards and is replaced by another parcel sweeping in from aloft. During the connect time with the surface, scalar transfers to or from the sources to the air parcel. Thus, the parcel has been enriched (depleted) with the scalar. Scalar turbulent exchange at the surface (vegetation) – atmosphere interface is therefore driven by the regular replacement of air parcels in contact with the sources (sinks). It was previously shown that this continuous renewal process is responsible for the majority of vertical transport (Gao et al., 1989; Lohou et al., 2000; Hongyan et al., 2004).

The renewal process is associated to an organized low-frequency flow (canopy-scale coherent structures). The *signature* of a coherent eddy motion, at a fixed measurement point, can be abstracted when the high-frequency measurement of the scalar is plotted versus time. Even measuring well above the canopy, the *signature* is visualized in the trace as a regular and low-frequency ramp-like (asymmetric triangle shape) pattern. Fig. 1a shows the ramp-like pattern in traces

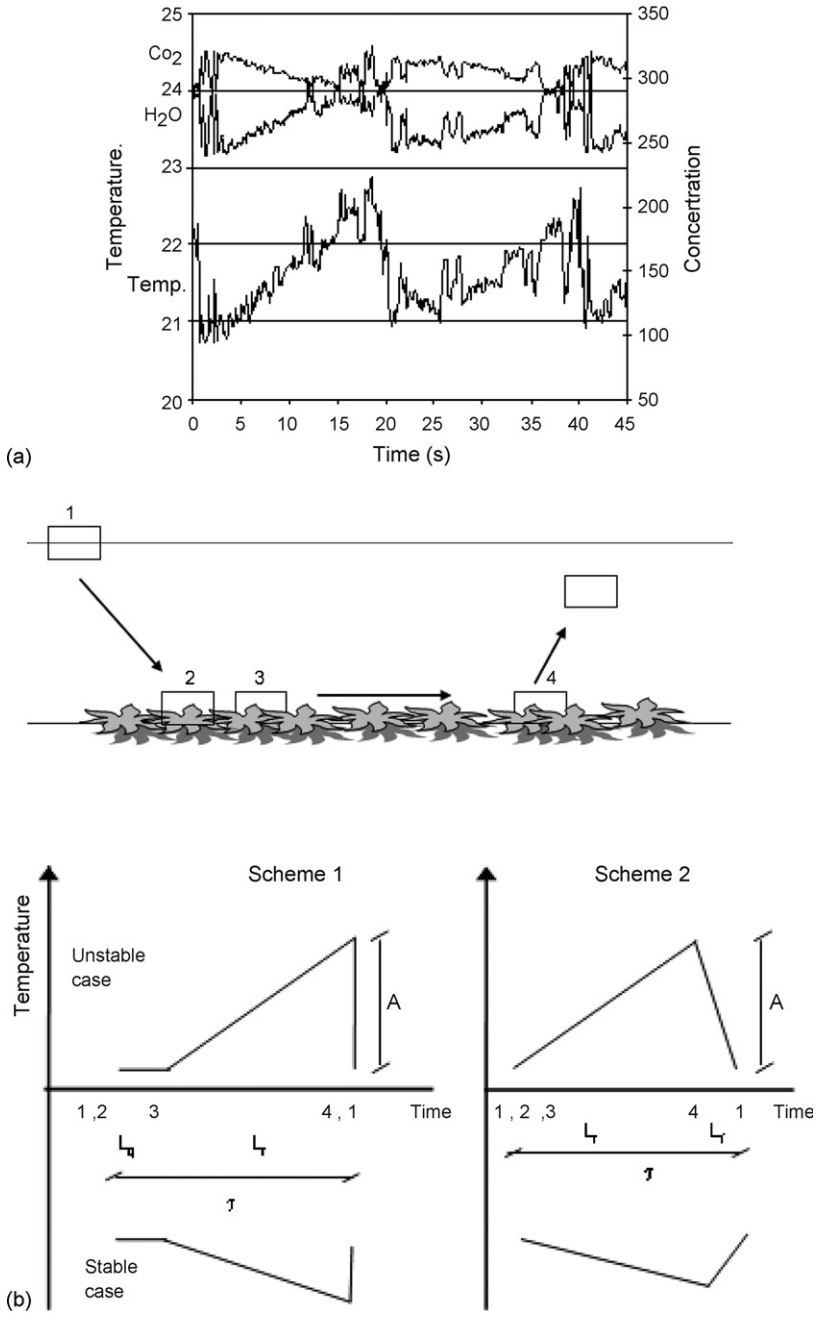

Fig. 1 – (a) Temperature (T in °C), water vapour concentration (H_2O in mmol m^{-3}), and carbon dioxide concentration (CO_2 in $\times 10^{-4}$ mol m^{-3}) versus time for a 45 s interval during a sample from 1330 to 1400 h on 14 April. For each scalar, two ramps are shown which have durations of about 20 s. The amplitudes are positive for temperature and water vapour concentration and negative for CO_2 concentration. (b) Air parcel diagram of the renewal process. The time course of the scalar concentration for the positions shown in the diagram are idealized in two air temperature ramp models. Scheme 1 assumes a quiescent period and a sharp instantaneous drop in temperature. Scheme 2 neglects the quiescent period and assumes a finite micro-front. L_r, L_q and L_f denote the warming, quiescent and micro-front periods, respectively. A is the ramp amplitude and τ is the total ramp duration.

for temperature, humidity and carbon dioxide over a short time period. Paw U et al. (1995) presented a diagram of the surface renewal process (Fig. 1b) and abstracted an ideal scheme for a ramp-like event in the trace (Scheme 1 in Fig. 1b). Chen et al. (1997a) presented a slightly different version (Scheme 2 in Fig. 1b) that neglects the quiescent period but includes a micro-front period instead of an instantaneous ejection. Whatever the model, a ramp is characterized by an amplitude, A_r, and period, τ. According to the diagram in Fig. 1b, the variation in scalar concentration versus time is Lagrangian during the time that the air parcel remains connected to the surface (i.e, $(L_q + L_r)$ and L_r for Schemes 1

and 2, respectively). Ideally, the different visual time course of the scalar between Fig. 1a and schemes in Fig. 1b produces the difference between the total time derivative (Lagrangian) and the partial time derivative (Eulerian) of the scalar concentration (Paw U et al., 1995). By denoting time and scalar concentration as t and c, respectively, and aligning the horizontal travel of the air parcel in the x-axis (no cross-horizontal flow in the y direction), the difference is

$$\frac{dc}{dt} - \frac{\partial c}{\partial t} = u\frac{\partial c}{\partial x} + w\frac{\partial c}{\partial z} \tag{3}$$

where u and w are the wind speed along the streamwise and z along the vertical direction at the fixed point where the data are measured. According to Katul et al. (1996), assuming an incompressible flow the differences in time are mainly attributed to high frequency eddies attached to the organized motion. Because the right-hand side in Eq. (3) is a local advective term driven by the smallest eddies it must never be associated with other higher scale advection-related processes such as lack of fetch as defined when using similarity theory. Based on scalar conservation within a volume and denoting the Lagrangian and Eulerian scalar sources as, S_L and S_E, respectively, the difference between S_L and S_E, assuming that molecular diffusion is negligible, is

$$S_E - S_L = c\left(\frac{\partial u}{\partial x} + \frac{\partial w}{\partial z}\right) \tag{4}$$

The two sources are the same when the flow is incompressible, but density variations may occur while the parcel is being enriched (depleted) with different scalars (Webb et al., 1980; Paw U et al., 2000). According to Eqs. (1) or (2), it is obvious that S_E averaged over time and depth $\langle S_E\rangle$ is the scalar source of interest. The main idea revolving around SR analysis for flux estimates is to evaluate S_L averaged in time and depth in the air parcel $d\langle c\rangle/dt = \langle S_L\rangle$, by extracting the time averaged coherent part in the trace (i.e., identifying the periodic ramp-like pattern in the trace after removing the high-frequency fluctuations). Therefore, assuming an air parcel with a volume V that covers the vertical extent of a source, the parcel sweeps to the surface where it (1) remains connected with the source until ejection, (2) is enriched with the scalar while in contact with the source, with no loss or gain of mass (or scalar) from the parcel top, and (3) is well mixed with negligible gradients and molecular diffusion. Then, the source S_L averaged in time and depth in a parcel with height, z, per unit area, A (i.e., $V = Az$), during the enrichment phase is

$$\frac{V}{A}\frac{d\langle c\rangle}{dt} = z\langle S_L\rangle = z\frac{A_r}{L_r} \approx z\langle S_E\rangle \tag{5}$$

Weighting Eq. (5) by the fraction of the total ramp duration (i.e., L_r/τ), the mean turbulent flux of scalar, $\overline{w'c'}$, at height, z, can be estimated as (Paw U et al., 1995)

$$z\frac{A_r}{L_r}\frac{L_r}{\tau} \approx \overline{w'c'} = (\alpha z)\frac{A_r}{\tau} \tag{6}$$

According to Eulerian scalar conservation equation, Eq. (6) is integrated from the ground to the top of the air parcel, z, and the storage and scalar flux from the ground is assumed negligible. In practice, the trace is recorded at height, z, which is at the top of the volume considered in the energy budget. Therefore, instrumentation placement at or above the canopy top is necessary. For sensible heat, $c = \rho C_P T$, where ρ and C_p are the density and specific heat of dry air at constant pressure and T is the air temperature. The parameter α is included to correct for all the assumptions in Eq. (6); in particular (1) vertical gradients are negligible and (2) the flow is incompressible. To simplify, earlier approaches assumed that the parameter α was a constant for fixed canopy characteristics and measurements at one height. Because thin layers are well mixed, measuring the trace at several heights within the source helps to overcome the first shortcoming. It, however, is sometimes physically impossible to measure at several layers within a canopy and it increases the cost. Several studies shown that α depends on the measurement level, Obukhov length and canopy architecture (Snyder et al., 1996; Katul et al., 1996; Castellvi, 2004). The following relationship was proposed for estimating α for sensible heat flux over the averaging period (Castellvi, 2004); its derivation was based on the one-dimensional (vertical) turbulent diffusion equation, similarity concepts, ramp model shown in Scheme 2 (Fig. 1b) and incompressible flow

$$\alpha = \begin{cases} \left[\frac{k}{\pi}\frac{(z-d)}{z^2}\tau u_* \phi_h^{-1}(\varsigma)\right]^{1/2} & (z-d) > z^* \\ \left[\frac{k}{\pi}\frac{z^*}{z^2}\tau u_* \phi_h^{-1}(\varsigma)\right]^{1/2} & h \le (z-d) \le z^* \end{cases} \tag{7}$$

In Eq. (7), d is the zero-plane displacement, z^* is the roughness sub-layer depth, h is the canopy height, u_* is the friction velocity, $k = 0.40$ is the Von Kármán constant, $\phi_h(\zeta)$ is the stability function for heat transfer (valid for any scalar) described below in Eq. (9), and ζ is an stability parameter defined as, $(z-d)/L_O$, with L_O being the Obukov length; defined by Businger (1988) as

$$L_O = -\frac{{u_*}^3}{kg\left(\overline{w'T_v'}\right)}T_v \tag{8}$$

where g is the acceleration due to gravity and T_v is the virtual temperature, which can be replaced with T in dry environments. The accepted formulation for $\phi_h(\zeta)$ was given by Foken (2006) and Högström (1988) as

$$\phi_h(\varsigma) = \begin{cases} (0.95 + 7.8\varsigma) & 0 \le \varsigma \le 1 \\ 0.95(1 - 11.6\varsigma)^{-1/2} & -2 \le \varsigma \le 0 \end{cases} \tag{9}$$

To overcome the second shortcoming, if the flow is not considered incompressible in an approximately constant pressure layer, flux corrections for the effect of density fluctuations may be addressed using the theory developed by Webb et al. (1980), the WPL correction, and Paw U et al. (2000).

3. Materials and methods

3.1. The site and climate features

The experimental site consisted of approximately 0.25 m tall rangeland grass. This is an AmeriFlux site located near Ione,

California, which is situated in the oak/grass savannah biome of eastern California in the foothills of the Sierra Nevada Mountains. The soil, climate, biome, and instrument set up at the site and surroundings were thoroughly described in Baldocchi et al. (2004) and Xu and Baldocchi (2004). Maximum temperatures during the growing season (winter and spring) were rarely above 15 °C and minimum temperatures never dropped below −5 °C. Freezing temperatures happened frequently, however, and their occurrence stymied growth of the grass and stomatal opening. During the summer, when the grass was dormant, maximum air temperature often exceeded 40 °C in the afternoon and dropped below 10 °C at night. The maximum soil moisture content occurred during the winter rainy season. After repeated winter rainstorms, the maximum soil moisture value in the upper 0.6 m was 0.31 $m^3\ m^{-3}$. After the rains stopped in the spring, vegetation progressively depleted moisture from the soil profile. By the start of the autumnal rains, the minimum soil moisture had dropped to about 0.09 $m^3\ m^{-3}$. The site, however, might experience lateral water flow because of its slightly convex topography. Soil texture was 29.5%, 58% and 12.5% of sand, silt and clay, respectively, and the soil bulk density was 1.43 (±0.125) g cm^{-3} (based on 27 samples from 0.05 to 0.3 m).

3.2. The field experiment

Field data were collected during 2002. The soil heat flux was measured as the mean output of three soil heat flux plates (model HFP-01, Hukseflux Thermal Sensors, Delft, The Netherlands). They were buried 0.01 m below the surface and were randomly placed within a few meters of the eddy covariance system. The gradual build up of plant matter changed the thermal properties of the upper layer. Consequently, heat storage was quantified in the upper layer by measuring the time rate of change in temperature using the method of Fuchs and Tanner (1967). Two probes were placed in the soil to sample soil temperature. Soil temperatures were measured with multi-level thermocouple probes. The sensors were spaced logarithmically at 0.02, 0.04, 0.08, 0.16 and 0.32 m below the surface. The net radiation was measured using a net radiometer ((NR Lite, Kipp and Zonen, Delft, The Netherlands) placed at 2 m height above the soil near the heat flux plates and thermocouple probes. The three wind speed components, air temperature, water vapor and CO_2 concentrations were recorded at 10 Hz.

The sonic anemometer (Windmaster Pro, Gill Instruments, Lymington, UK) was placed at 2.0 m above the ground and an open-path (LI-7500, LICOR, Lincoln, NE) infrared absorption gas analyser (IRGA) was located at the same height with 0.15 m separation from the sonic sensor. The fast response IRGA was calibrated every 3–4 weeks against gas standards. The calibration standards for CO_2 were traceable to those prepared by NOAA's Climate Monitoring and Diagnostic Laboratory. The output of the water vapor channel was referenced to a dew point hygrometer (LI-610, Licor, Lincoln, NE). The calibration zeros and spans showed negligible drift. In-house software was used to process the measurements into half-hourly flux densities using the Reynolds decomposition technique. The software removes electrical spikes (Vickers and Mahrt, 1997) and rotates the coordinate system to force the mean vertical velocity to zero. Some studies (Paw U et al., 2000; Finnigan et al., 2003) have recommended using the planar rotation method of instead of classic coordinate rotation method to compute flux covariance. The calculations revealed that the classic coordinate rotation method produced similar results as the planar rotation method. This occurred because the mean angle of rotation for the grassland was less than 1.3°. Computations of the flux covariance transfer functions (Moore, 1986) were made to guide the positioning of sensors in the field. Overall transfer correction factors were less than a few percent. Considering uncertainties with applying the transfer functions, they were not applied in this experiment. The Kristensen et al. (1997) correction was not implemented because distance separation (s = 0.15 m) over the measurement height (z = 2 m) was small (s/z = 0.075). According to Paw U et al. (2000), the work of expansion under constant pressure, which is 0.076 times the latent heat flux, was included in the sensible heat flux. The WPL corrections were applied to the scalar covariance that was measured with the open-path sensor.

Numerical footprint calculations performed with a Lagrangian model (Baldocchi, 1997) indicate that the fetch was well within the flux footprint during near neutral and unstable thermal stratification. To account for stationary conditions, the test proposed in Foken and Wichura (1996) was applied at the level of 20%.

3.3. Procedure for solving Eq. (6)

Ramp dimensions for each scalar trace were determined, as described in Appendix A, using three time lags because minor differences occur for slightly greater time lags than that which maximizes the third order structure function (Chen et al., 1997b). By invoking similarity, the parameter γ in Eq. (A.5) was set to $\gamma = 1.1$ for all three scalars. Because the interdependence in Eqs. (6)–(9), an iterative method was used for simultaneously solutions. As a consequence, two other equations were employed to provide estimates for the zero-plane displacement and friction velocity. The procedure to solve Eq. (6) for each scalar is shown in Appendix B. The work of expansion under constant pressure was included in the sensible heat flux correction and the WPL correction was applied for other fluxes.

3.4. The database and performance evaluation

Table 1 shows the mean and standard deviation for air temperature, vapor pressure deficit and surface fluxes corresponding to four different datasets. Two datasets were formed from samples gathered under unstable surface-layer atmospheric conditions. The dry period dataset corresponds to day of year 160 until 298 when the half-hourly EC latent heat fluxes never exceeded 65 W m^{-2}, having a mean value during daylight time of 10 W m^{-2}. The remaining days define the humid period. As shown in Table 1, the energy partitioning of the available net surface energy was remarkably distinct for these two datasets. For the humid period, sensible and latent heat fluxes were similar because the high soil water content. For the dry period the soil water was depleted, grass was stressed and went dormant, and the albedo increased.

Table 1 – Number of half-hour samples (*N*), mean air temperature (*T*) and vapor pressure deficit (VPD) during the indicated atmospheric conditions

Subsets	N	T (°C)		VPD (kPa)		H_{EC} (W m^{-2})		L_wE_{EC} (W m^{-2})		F_{pEC} (μmol m^{-2}s^{-1})		$R_n - G$ (W m^{-2})	
		Mean	S.D.	Mean	S.D.	Mean	S.D.	Mean	S.D.	Mean	S.D.	Mean	S.D.
Unstable, wp	935	22.5	5.5	1.9	0.97	170.2	93.7	109.0	67.7	−18.9	7.5	315.4	128.5
Unstable, dp	1745	27.4	6.1	2.8	1.45	211.0	99.6	9.9	9.5	−15.9	7.2	241.3	115.3
Stable, $R_n - G < 0$	1407	19.0	3.8	1.2	0.86	−19.1	11.5	0.0	4.7	2.5	1.8	−24.4	13.0
Stable, $R_n - G > 0$	338	23.0	4.6	1.8	0.82	−12.9	10.2	14.7	28.8	1.9	2.1	17.5	24.1

Mean and standard deviation (S.D.) of EC measured surface fluxes for sensible heat flux (H_{EC}), latent heat flux (L_wE_{EC}), carbon dioxide flux (F_{pEC}), and net radiation minus soil heat flux density ($R_n - G$) by atmospheric conditions. The subset indicators wp and dp denote the wet and dry periods, respectively.

Therefore, during the dry period, most of the available net surface energy contributed to positive (upward) sensible heat flux. Regardless of the study period, the carbon dioxide flux was similar.

Two other datasets were formed from samples gathered under stable atmospheric conditions. One stable-case dataset included periods when $R_n - G$ was positive, which corresponded to periods close to sunrise, sunset and late afternoon. During these periods, the grass was transpiring with a subsequent cooling of the adjacent atmospheric sub-layer, which led to negative sensible heat flux. For this dataset, the available net surface energy and sensible heat flux contributed to a positive late afternoon maximum L_wE = 145 W m^{-2}. The other stable-case dataset corresponded to nighttime periods with negative $R_n - G$ values and small H and L_wE.

Linear regression analysis (LRA) and the root mean square error, rmse, were used to analyze the performance of flux estimates and closure of the surface energy-balance. Caution is needed when evaluating the *LRA*, however, because it assumes that the independent variable is free of random errors. Therefore, following Marth (1988), the ratio ($D = \Sigma y/\Sigma x$), which is the sum of the fluxes (Σy) over the sum of fluxes taken as a reference (Σx), was also determined as an evaluation parameter. The coefficient D is used to determine the percentage (p) being over- or under-estimated ($p = 100 \times (1 - D)$). The value D also gives an integrated evaluation of the bias on daily, monthly, and seasonal time scales by averaging out random errors in the half-hourly estimates (i.e., the bias is $(D - 1)$ times the mean value determined from the observations). For closure of the energy-balance, taking $(R_n - G)$ as a reference in Eq. (2), it is shown that D typically ranges within the interval $0.7 < D < 1$ (Twine et al., 2000) with an annual mean of D = 0.84 for different climates and surfaces (Wilson et al., 2002).

4. Results

Hereafter, flux estimates from SR analysis and the EC method will be denoted using sub-indexes SR and EC, respectively. Table 2 shows the *LRA*, rmse, and D for H_{SR}, L_wE_{SR} and F_{pSR} versus H_{EC}, L_wE_{EC} and F_{pEC}, respectively. The L_wE_{EC} and L_wE_{SR} were compared against $R_n - G - H_{EC}$, and Table 3 shows the performance (*LRA*, rmse and D) in closing the energy-balance (Eq. (2)), where $R_n - G$ was the independent variable. Carbon dioxide flux was negligible ($-14 < L_pF_p < 5$ W m^{-2}) and was not included in the closure equation.

4.1. *Unstable cases*

Table 2 shows a high correlation between H_{SR} and H_{EC}. During the wet and dry season, H_{SR} analysis was higher than H_{EC} by 3% and 5%, respectively. For latent heat flux, however, a contrasting performance was found depending on atmospheric conditions. For the wet period, L_wE_{SR} was higher than L_wE_{EC} by 18%. When either L_wE_{EC} or L_wE_{SR} were compared with $R_n - G - H_{EC}$, the correlations were high and the intercepts were small; however, L_wE_{EC} and L_wE_{SR} underestimated $R_n - G - H_{EC}$ by 25% and 11%, respectively. Comparing with the equation $L_wE = R_n - G - H_{EC}$, the bias determined for L_wE_{EC} and L_wE_{SR} were −36 W m^{-2} and −15 W m^{-2}, respectively. If one considers that $R_n - G - H_{EC}$ is a reasonable estimate of the actual latent heat flux, L_wE_{SR} performed better than L_wE_{EC} with a higher rmse (Table 2). For the dry period, L_wE_{SR} and L_wE_{EC} were dissimilar, but they had a high rmse (Table 2) and showed a poor correlation when compared with $R_n - G - H_{EC}$. Latent heat fluxes were small and likely on the same order of magnitude as the measurement errors. In general, well-formed ramps were observed for air temperature but not for water vapor traces during dry conditions. During the humid period, well-formed ramp traces of both air temperature and water vapor concentration were observed, which explains why the L_wE_{SR} performance was good for the wet period. Good correlations indicate that SR estimates captured a high portion of the actual flux variability because the EC directly measures the turbulent flow. For carbon dioxide flux, correlation was good regardless of the wetness conditions. SR analysis (F_{pSR}) predicted fluxes that were 12% and 7% higher than eddy covariance (F_{pEC}) flux during the wet and dry period, respectively (Table 2). By invoking similarity with water vapor, one would likely presume that F_{pSR} is more reliable than F_{pEC} since this happened with L_wE using $R_n - G - H_{EC}$ as a reference.

Except for L_wE during the dry period, SR analysis always estimated higher than the EC method; however, both methods had better agreement for sensible heat flux than for latent heat and carbon dioxide flux (Table 2). Arguments to explain the different performance between scalars are discussed below.

The SR method escapes problems resulting from IRGA and sonic anemometer separation and time delay, but these

Table 2 – Regression, rmse, and D statistics for SR analysis versus EC method by independent (Indep.) variable

Indep. variable	H_{EC}					L_wE_{EC}					$(R_n - G - H_{EC})$[a]					$(R_n - G - H_{EC})$[b]					F_{pEC}				
Subsets	b	a	R^2	rmse	D	b	a	R^2	rmse	D	b	a	R^2	rmse	D	b	a	R^2	rmse	D	b	a	R^2	rmse	D
Unstable, wp	1.00	12	0.85	41	1.03	1.07	11	0.88	34	1.18	0.70	6	0.82	52	0.75	0.84	8	0.87	35	0.89	1.09	−0.4	0.93	3.3	1.12
Unstable, dp	0.97	17	0.85	42	1.05	0.62	3	0.40	8	0.92	0.09	7	0.09	35	0.32	0.11	6	0.10	35	0.30	1.06	−0.2	0.97	1.8	1.07
Stable, $(R_n - G) < 0$	0.45	−6	0.30	10	0.82	0.57	0	0.40	3	−9.0	0.63	3	0.68	13	0.00	0.07	0	0.03	12	−0.04	0.81	0.5	0.70	1.0	1.00
Stable, $(R_n - G) > 0$	0.31	−8	0.11	11	0.93	0.50	0	0.76	18	0.58	0.94	−10	0.74	20	0.48	0.56	−9	0.63	27	0.24	0.76	0.1	0.62	1.4	0.82

Statistics include the slope (b), intercept (a), coefficient of determination (R^2), and the root mean square error (rmse). The statistic D is the ratio of the sums of the dependent over the independent variables. Units are W m^{-2} for H_{EC}, L_wE_{EC}, and $R_n - G - H_{EC}$ and the units are μmol m^{-2} s^{-1} for F_{pEC}. The subset indicators wp and dp denote the wet and dry periods, respectively. [a]L_wE_{EC} and [b]L_wE_{SR} were the dependent variables, respectively.

factors did not play a key-role for this experiment. Although not shown, the Moore (1986) corrections did not improve the statistics. Other source of errors (e.g., insufficient fetch, lack of homogeneity and calibration) are also unlikely to play a key-role. Sensor maintenance and data quality were carefully controlled. A source of error might be the correction implemented for an incompressible flow. The WPL flux correction for latent heat and carbon dioxide requires the scalar covariance with other scalars, and thus the error is propagated from one scalar to another.

Linear regression analysis comparing mean vertical velocities due to density fluctuations determined from SR analysis and the EC method (as the independent variable) showed that slopes differed within 2%, intercepts were negligible, and coefficients of determination were 0.95. With regard to the closure of the energy-balance, Table 3 provides an integrated evaluation of the sensible and latent heat flux estimates. However, caution is advised when evaluating shortcomings or problems related on turbulent flux estimates using closure. The lack of EC closure is a historical problem because it cannot be explained even assuming that all the instrument shortcomings involved in the EC method are perfectly corrected (Marth, 1988; Laubach and Teichmann, 1999; Kanda et al., 2004; Foken et al., 2006; Beyrich et al., 2006; Inagaki et al., 2006; Steinfeld et al., 2007; Mauder et al., 2007). Moreover, accurate $(R_n - G)$ measurements are crucial, and the measurement error is highly sensor dependent (Kohsiek et al., 2007).

In this experiment, homogeneous surfaces were favorable to diminish the total error, but the R_n instrument error cannot be evaluated from our experiment. Twine et al. (2000), using a CNR1 Kipp and Zonen sensor to measure R_n found that a realistic measurement error for $(R_n - G)$ was about 6% over grazed surfaces. For this experiment, the error for $(R_n - G)$ was probably similar or slightly higher than 6% because a less accurate net radiation sensor was used.

Table 3 shows that regardless of the weather conditions, $H_{EC} + LE_{EC}$ underestimated the available net surface-energy by 10% for all of the data. Such imbalance is unlikely to be attributed to a 10% error in $(R_n - G)$. According to Baldocchi et al. (2004) and Wilson et al. (2002), such an EC underestimation is moderate. For SR analysis, however, the $H_{SR} + L_wE_{SR}$ estimates provided D coefficients closer to one than $H_{EC} + L_wE_{EC}$. During the dry period, closure of the EC method had a smaller rmse than the SR analysis, but the rmse was similar during the wet period (Table 3). When the WPL correction was not applied for the SR latent heat flux calculations, the closure had slopes that were about 3% lower while intercepts, correlations, and rmse were nearly the same. The corresponding D coefficients were 0.97 and 0.92 for the wet and dry periods, respectively. Therefore, the SR analysis without the WPL correction still provided a better closure than the EC method.

Fig. 2a and b show $H_{EC} + L_wE_{EC}$ and $H_{SR} + L_wE_{SR}$ versus $R_n - G$, respectively. For $R_n - G > 125$ W m^{-2}, $H_{EC} + L_wE_{EC}$ underestimated $R_n - G$; whereas, $H_{SR} + L_wE_{SR}$ estimates were roughly equal to $R_n - G$. The bias observed in Fig. 2a for the EC method could partly be associated with a consistent loss of flux by local convection due to a small non-zero mean vertical velocity ($\overline{w}$) induced by topography. For the EC method, rotation is required to force the mean convective flux to zero,

Table 3 – Energy-balance closure

Dependent variable:	$H_{EC} + L_wE_{EC}$					$H_{SR} + L_wE_{SR}$				
Subsets	b	a	R^2	rmse	D	b	a	R^2	rmse	D
Unstable, wp	0.85	12	0.91	53	0.89	0.88	38	0.84	51	0.99
Unstable, dp	0.87	9	0.95	35	0.91	0.90	15	0.87	43	0.96
Stable, $(R_n - G) < 0$	0.55	−5	0.41	11	0.79	0.33	−6	0.21	15	0.63
Stable, $(R_n - G) > 0$	1.12	−17	0.79	21	0.10	0.51	−14	0.57	27	−0.3

($H + L_wE$) versus the net surface-energy ($R_n - G$). Statistics include the slope (b), intercept (a), coefficient of determination (R^2), and the root mean square error (rmse). The statistic D is the ratio of the sums of the dependent over the independent variables. Units are W m^{-2}. The subset indicators wp and dp denote the wet and dry periods, respectively.

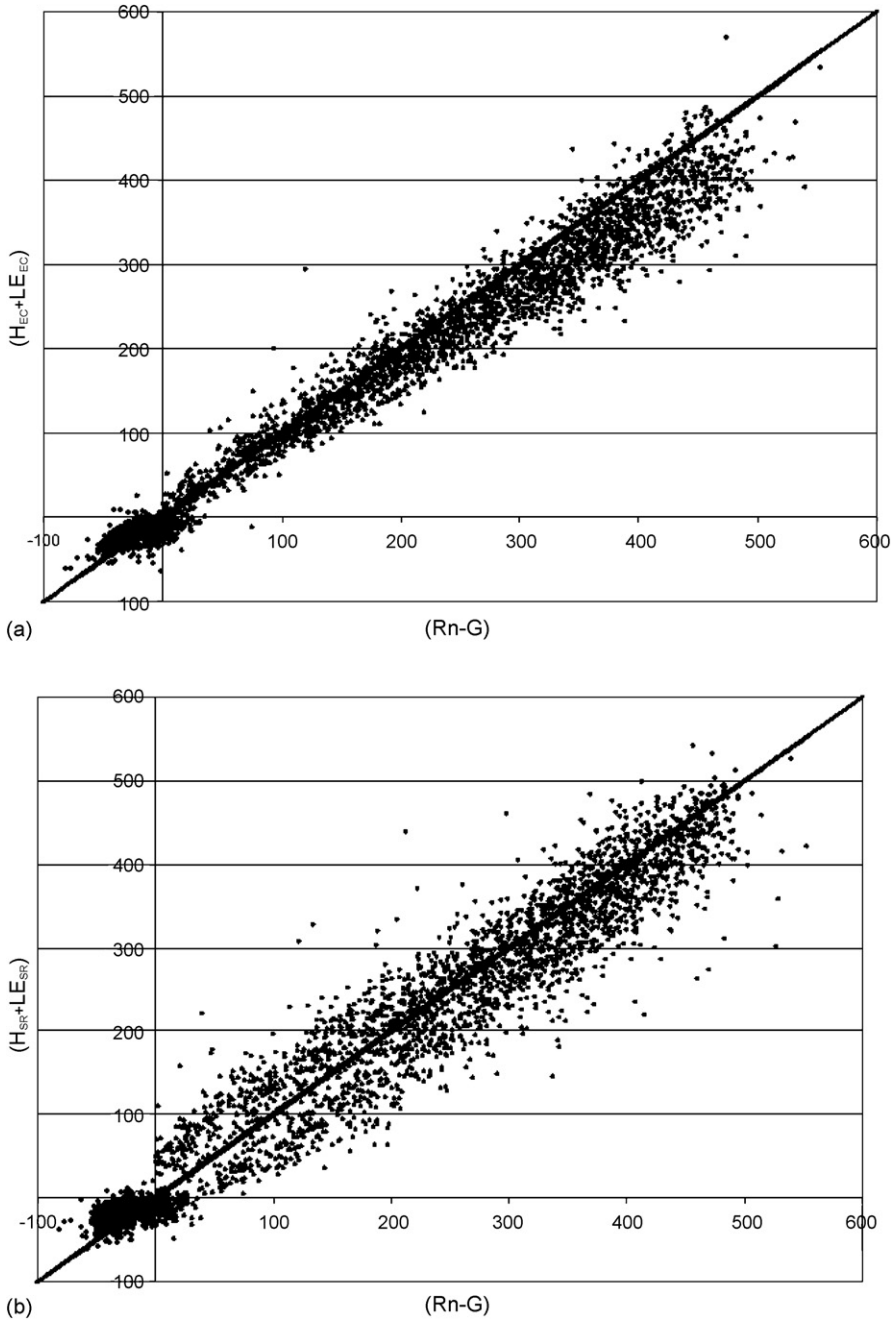

Fig. 2 – $H + L_wE$ estimates versus measured $R_n - G$ for all the data using (a) the EC method and (b) the SR analysis.

but it may be induced by mesoscale circulations. According to Mortensen (1994), $\overline{w} = 0.001\,\mathrm{ms}^{-1}$ are not detectable by eddy correlation systems and this may explain the closure when the EC imbalance is moderate (Laubach and Teichmann, 1999).

For SR analysis, a non-zero $\overline{w}$ (detectable or not by a sonic anemometer) might cause an underestimate of the actual flux. The SR method assumes that there is no mass or heat loss through the parcel top. The amount of scalar loss from the parcel top should be negligible for small $\overline{w}$ for high ramp frequency and large volumes of renewed air parcels. For such conditions, the mean vertical displacement of the scalar, while the parcel is connected to the surface, $(\overline{w}\tau)$, is negligible when compared with the parcel height (z). Assuming $\overline{w} \approx 0.001\,\mathrm{m\,s}^{-1}$, $(\overline{w}\tau)/(z)$ was on the order of 10^{-2}, which is within the instrumental measurement error for vertical placement above the ground. Though small mean convection may have minor influence on the assumptions made in Eq. (6), in principle, SR analysis cannot account for mean convective flux. The latter is associated with larger than canopy scale eddy motion. Therefore, a small $\overline{w}$ only can induce to SR imbalance.

Finnigan et al. (2003) suggested computing block flux averages for several hours to account for low frequencies. However, block averages from half-hourly to three hours showed little improvement for the D coefficient (i.e., the improvement with respect the D values was within 3% in Table 3). For SR analysis block-averaging longer than half hour is not recommended because Eq. (6) is derived from SR theory in conjunction with the analysis to clarify those ramps in the scalar trace that are associated to canopy-scale coherent structures. Half-hourly traces are adequate for such task. In addition, Eq. (7), which eliminates the need for SR calibration, is highly dependent on stability conditions (Castellvi, 2004). Moreover, similarity based-relationships (Eq. (9) and Appendix B) were obtained from half-hour samples (Högström, 1988; Foken, 2006).

According to Högström (1988), the expression used for $\phi_h(\zeta)$, Eq. (9), produced the best fit for different experiments and accomplish the following standard, $k = 0.40$ and $\phi_h(\zeta = 0) = 0.95$. By invoking similarity, Eq. (9) is a *universal* relationship. After standardization of different $\phi_h(\zeta)$ expressions obtained in different experiments, Eq. (9) give results within 10%. SR flux estimates were also determined using the modified $\phi_h(\zeta)$ Dyer (1974) expression, valid for $k = 0.41$, and a refined Eq. (9) to impose $\phi_h(\zeta = 0) = 1$, which is more realistic from a physical point of view (Högström, 1988). It was found that the new SR flux estimates were about 4% higher (Dyer's case) and about 2% lower (Högström's case for $\phi_h(\zeta = 0) = 1$) with respect Eq. (9) which is Högström's case for $\phi_h(\zeta = 0) = 0.95$. The Dyer's case resulted in a excellent closure (i.e., coefficient D was 1.00 for the wet and dry periods) while Högström's case for $\phi_h(\zeta = 0) = 1$ produced a slightly higher imbalance (i.e., coefficient D for the wet and dry periods were 0.97 and 0.94, respectively). According to the D variability on $\phi_h(\zeta)$, it is therefore reasonable to assume that SR analysis did a better closure than EC because Eq. (9) underestimated $\phi_h(\zeta)$ at the site. Eq. (7) predicts higher α parameters and consequently higher fluxes. We note however that, although underestimation of the actual $\phi_h(\zeta)$ may explain the D values higher than one in Table 2 and closure in Table 3, it cannot explain why SR and EC showed closer results for temperature than for the other two scalars. Because SR flux estimates are sensitive to variations in Eq. (9), some degree of dissimilarity between scalars can explain the different SR and EC energy partitioning and performance. Dissimilarity implies that stability functions for scalar transfer are different and unknown (i.e., whatever the scalar, Eq. (9) does not necessarily hold).

It is well recognized that dissimilarity may occur under the influence of advection (Lee et al., 2004), and that regional advection regularly forms in the San Joaquin Valley of California from late spring to early fall. Based on a second-order closure model, Warhaft (1976) demonstrated that the ratio of the similarity relationships for scalar c, $\phi_c(\zeta)$, and for temperature (heat) within an unstable surface layer is given by

$$\frac{\phi_c(\zeta)}{\phi_T(\zeta)} = 1 - \frac{1}{2}\frac{g}{\overline{w'^2}}\frac{\overline{T'^2}}{\overline{T}}\frac{1}{(\mathrm{d}T/\mathrm{d}z)}\left(R_{Tc}\frac{R_{wT}}{R_{wc}} - 1\right) \quad (10)$$

where R_{xy} is the coefficient of determination between variables x and y. Given that, $\overline{w'^2}$, $\overline{T'^2}$, and $-\mathrm{d}T/\mathrm{d}z$ are greater than zero for $\zeta < 0$, Eq. (10) predicts similarity when $R_{wT}/R_{wc} = 1/R_{Tc}$. Fig. 3a and b show $(R_{Tq}R_{wT}/R_{wq})$ and $(R_{TCO_2}R_{wT}/R_{wCO_2})$ versus H_{EC} for the wet and dry periods, respectively. High values near neutral conditions were not included in Fig. 3 because they distorted the vertical axis, and plots of $\phi_c(\zeta)/\phi_T(\zeta)$ are not shown because dT/dz was not available. Fig. 3a and b included $H_{EC} = 0\,\mathrm{W\,m}^{-2}$ in the abscissa axis as the lowest limit, but Eq. (10) only accounts for $H > 0$. For the wet period, Fig. 3a shows that similarity for all three scalars approximately holds when sensible heat flux is relatively high ($H_{EC} > 175\,\mathrm{Wm}^{-2}$). Otherwise, $\phi_T(\zeta) > \phi_c(\zeta)$ for most samples. This agrees with theory based on a diffusion originated by dual sources, which predicts $\phi_T(\zeta) > \phi_q(\zeta)$ at sites influenced by regional advection during periods where the surface sub-layer is under unstable conditions (Lee et al., 2004) and with the idea that dissimilarity shows up when, in the surface layer fluxes generated by sources located in the surface become on the same order as non-locally created fluxes, such as those generated by entrainment (De Bruin et al., 1999). With regard to the energy partitioning, it is reasonable to assume that part of the EC imbalance shown in Table 3 can be attributed to underestimation of the actual sensible heat flux. Hence, $R_n - G - H_{EC}$ results in an overestimation of the actual L_wE. For the wet period, this suggests that the 11% underestimation when L_wE_{SR} was compared to $R_n - G - H_{EC}$ (Table 2) seems to be an upper limit. Therefore, L_wE_{SR} would be useful for different purposes such as irrigation and model calibration. The degree of dissimilarity for water vapor and carbon dioxide versus temperature was comparable (Fig. 3a), which suggests that the SR carbon dioxide fluxes were also reliable for the wet season. Based on experiments carried out over near ideal sites (homogeneous and flat extend terrain), Twine et al. (2000) concluded that when the energy-balance closure is not achieved, the EC method underestimates the latent heat and carbon dioxide fluxes by the same factor. Accordingly, if $E_{EC}/E = F_{pEC}/F_p$ is valid, the ratio of D coefficients for latent heat and carbon dioxide fluxes (Table 2) indicates that underestimation for the SR latent heat flux (i.e, L_wE_{SR}/L_wE) is 1.05 times the underestimation for carbon dioxide (F_{pSR}/F_p). If one considers $L_wE_{SR}/L_wE \geq L_wE_{SR}/(R_n - G - H_{EC}) = 0.89$ (Table 2),

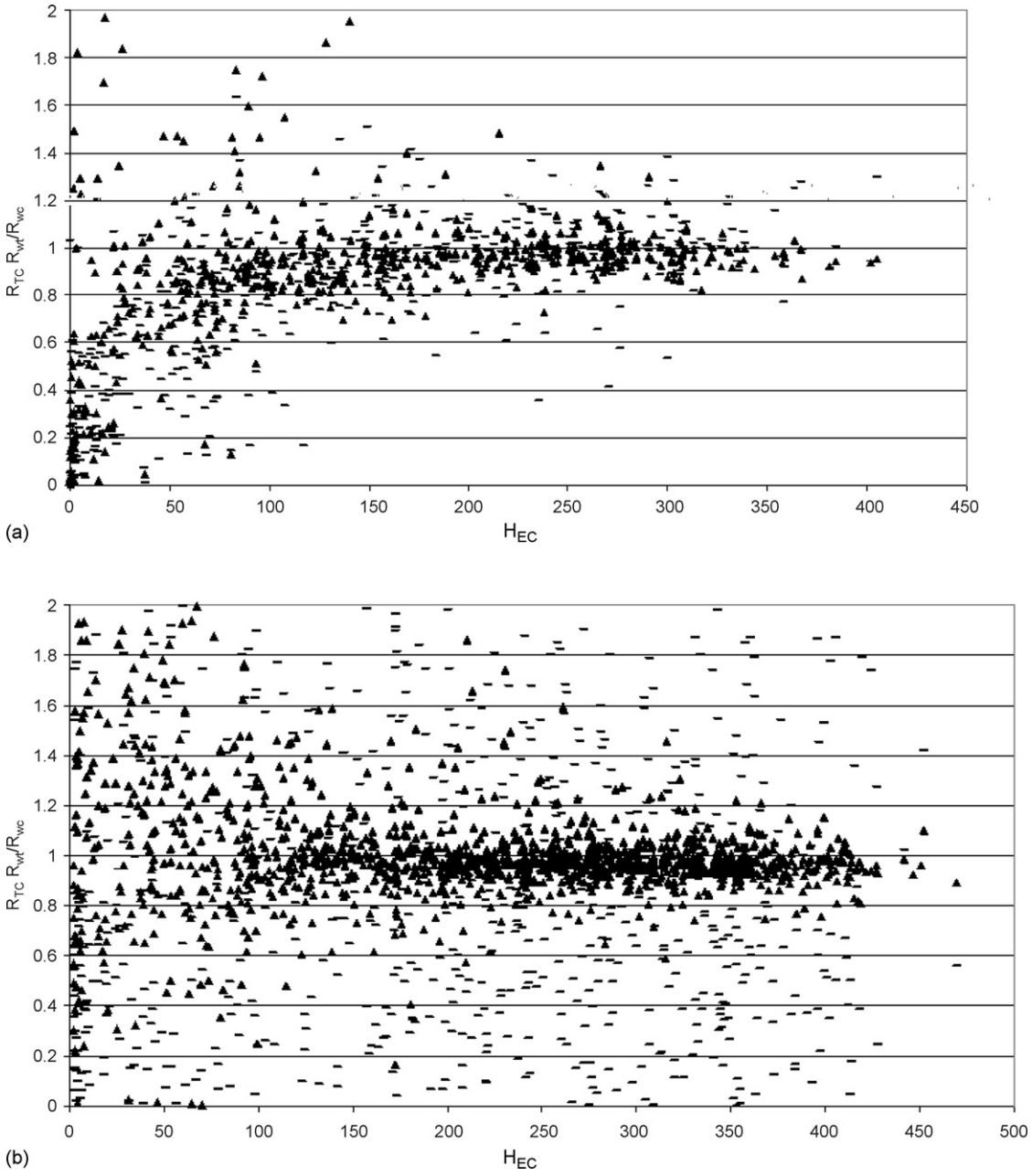

Fig. 3 – $R_{Tq}R_{wT}/R_{wq}$ (dash) and $R_{TCO_2}R_{wT}/R_{wCO_2}$ (triangle) versus H_{EC} in W m^{-2} for (a) the wet period and (b) the dry period.

then $F_{pSR}/F_p = 0.89/1.05$ indicates that an upper limit for the F_{pSR} underestimation was about 15.5%, which is substantially lower than the $F_{pEC}/F_p = E_{EC}/E$ upper limit underestimation of 25% according to D coefficient for $L_wE_{EC}/(R_n - G - H_{EC})$.

For the dry period, Fig. 3b shows that similarity for temperature and carbon dioxide roughly held for part of the day ($H_{EC} > 100$ W m^{-2}) than for the wet period. This explains why H_{SR} and H_{EC} had similar performance as F_{pSR} and F_{pEC} for the dry period (i.e., D coefficients in Table 2 were 1.05 and 1.07 for sensible heat and carbon dioxide, respectively). Sources for water vapor were exhausted and therefore humidity was absolutely uncorrelated with respect the other two scalars during the dry season, which induces dissimilarity (McNaughton and Laubach, 1998). Regardless that L_wE_{EC} values fall mostly within the measurement error, it is obvious that the SR latent heat flux cannot be assumed realistic since Eq. (9) is absolutely uncertain for water vapor under such dry environment. Because the SR sensible heat flux is considered reliable (Tables 2 and 3), it also applies for the SR carbon dioxide flux since $\phi_T(\zeta) \approx \phi_{CO_2}(\zeta)$ for most of the day.

For moderate EC imbalance, Twine et al. (2000) suggested that a reasonable way to refine the estimated EC fluxes is to force closure by assuming that the measured Bowen ratio, $\beta = H/L_wE$, is valid. The Bowen Ratio Energy Balance (BREB) method is described in Brutsaert (1988). Sensible and latent heat flux estimates obtained by combining Eq. (2) and the EC Bowen ratio, $\beta_{EC} = H_{EC}/L_wE_{EC}$ are denoted as $H_{BREB\text{-}EC}$ and $L_wE_{BREB\text{-}EC}$, respectively. Similarly, fluxes for SR analysis

determined from Eq. (2) and β estimated as, $\beta_{SR} = H_{SR}/L_wE_{SR}$ are denoted as $H_{BREB\text{-}SR}$ and $L_wE_{BREB\text{-}SR}$, respectively. The BREB-EC flux estimates were used as the independent variable for comparisons. For the wet period linear regression showed that the sensible heat flux $H_{BREB\text{-}SR} = 0.985H_{BREB\text{-}EC} - 10$ with $R^2 = 0.975$ and $H_{SR} = 0.92\ H_{BREB\text{-}EC} - 1$ with $R^2 = 0.86$. For latent heat flux regressions, $L_wE_{BREB\text{-}SR} = 1.09L_wE_{BREB\text{-}EC} - 2$ with $R^2 = 0.98$ and $L_wE_{SR} = 1.08L_wE_{BREB\text{-}EC} - 7$ with $R^2 = 0.92$. Regardless of whether the dependent variable was BREB-SR or SR, all of the slopes fell within 9% with respect the unity, intercepts were small, and the coefficient of determination was high.

If $\beta \approx \beta_{EC}$ from the BREB-EC, it implies that $H \approx pH_{EC}$ and $L_wE \approx pL_wE_{EC}$, where p is a known portion of the energy component. Even at ideal sites such assumption may not be true since we do not know the role of the large eddies for heat and moisture in the imbalance. Regardless, the BREB-EC method is likely the preferred micrometeorological method used in agronomy (Twine et al., 2000; Drexler et al., 2004), and the BREB-SR method and SR analysis performed nearly the same as the preferred EC method for both sensible heat and latent heat fluxes (Fig. 3a). The performance is also valid for carbon dioxide. The SR and EC Bowen ratios were similar, $\beta_{SR} = 0.90\beta_{EC} + 0.00$ with $R^2 = 0.89$. Therefore, the Bowen ratio can be estimated using SR analysis taking measurements at a single level which corroborates the results shown in Castellvi et al. (2006b) over a rice field with a limited fetch and a short dataset. For the dry period β_{EC} is considered meaningless since most of the L_wE_{EC} fell within the measurement error. In this case, although β_{SR} and β_{EC} showed poor correlation, the Bowen ratios were large and $H_{BREB\text{-}SR} = 1.00H_{BREB\text{-}EC} + 2$ with $R^2 = 0.99$. For SR analysis, $H_{SR} = 0.89\ H_{BREB\text{-}EC} + 17$ with $R^2 = 0.85$, but the H_{SR} underestimation seems unimportant because the large Bowen ratios likely inflated the sensible heat flux for $H_{BREB\text{-}EC}$. An underestimation of about 10% for sensible heat flux is still good for field applications such as the estimation of evapotranspiration ($R_n - G - H_{SR}$) for irrigation schedules.

4.2. *Stable cases*

When $R_n - G$ was positive, the L_wE_{EC} values were positive up to 145 W m^{-2}, but 85% of the samples had $L_wE_{EC} < 30$ W m^{-2}. Approximately 87% of the samples had $H_{EC} > -20$ W m^{-2} and 64% of the samples had $H_{EC} > -10$ W m^{-2}. For negative $R_n - G$, 99% of the samples had $L_wE_{EC} > -25$ W m^{-2} and the 67% had $H_{EC} > -25$ W m^{-2}. When fluxes are small, ramps in traces are not-well formed and therefore SR analysis is not applicable. On the other hand, errors made by the EC method when measuring small fluxes can be large. Therefore, the most important statistic to consider for SR evaluation in Tables 2 and 3 is the coefficient of determination. As expected, SR analysis showed better correlations when fluxes where higher. For carbon dioxide the correlations were high and for latent heat flux, correlations were good during daylight for both L_wE_{EC} and $R_n - G - H_{EC}$.

5. Summary and concluding remarks

This paper reports on an experiment to evaluate the energy-balance closure and CO_2 flux estimates using surface renewal (SR) analysis. Data were collected over rangeland grass and analyzed for different ranges of net radiation minus soil heat flux ($R_n - G$) during the late fall, winter, and spring (wet) period and during the remainder of the year (the dry period), in the Sierra Nevada Mountain foothills in California.

During unstable atmospheric conditions, the SR analysis and the EC method gave similar results for H. The latent heat flux measurements were highly correlated during the wet season. For carbon dioxide flux, correlations were also high regardless of the wetness conditions. Based on a long-term evaluation to balance errors, SR analysis had good closure. The latter was due to higher SR than EC fluxes. For all the data, SR analysis produced energy flux densities that were about 4%, 18% and 10% higher than the EC method for sensible heat, latent heat and carbon dioxide fluxes, respectively. Good correlation between the EC methods indicates that SR analysis was able to capture most of the actual flux variability. Because most of the fluxes associated with coherent structures can be detected with the EC method (Thomas and Foken, 2007), it is expected that SR analysis and the EC method will exhibit similar performance. Different potential uncertainties involved in surface-atmosphere scalar transfer processes makes it difficult to prove or explain why SR analysis: (1) gave a better closure than the EC method and (2) exhibited scalar differences when compared with the EC method. The difficulty would be substantially reduced if one could perfectly address all the instrumental shortcomings. Some arguments indicate that differences might be attributed to dissimilarity between scalars. Non-similarity by itself explains the different SR and EC performance for sensible heat and the other fluxes, and Eq. (9) might underestimated $\phi_h(\zeta)$ at a site. The latter was not proven in this study because profiles are required and the site is not a flat extend terrain that is free of advection influences. Analysis of potential error indicates that the similarity assumptions made in Eq. (7) maybe crucial for understanding the results shown in Tables 2 and 3. Errors associated to WPL corrections and assumptions invoked in SR such as mass loss from the top of the air parcel appeared to have less influence. SR analysis provided reliable estimates of the Bowen ratio. The two major implications are (1) SR analysis provided a reliable energy partitioning, and (2) when ($R_n - G$) is available the BREB-SR method results are good. The Bowen ratio can be estimated from measurements at a single level ($\beta_{SR} = (\rho C_p/L_w)(\tau_T/\tau_q)^{1/2}(A_T/A_q)$) and wind speed is not required as input. Subsequently, calculations and estimation of different canopy parameters, as shown in Appendix B, are avoided.

For stable atmospheric conditions, samples passing the quality control were generally near neutral atmospheric stability. Fetch requirements were more demanding for stable cases, and around dawn and dusk are periods of unsteady conditions. Since small fluxes are more affected by errors and, on gentle slopes, scalars may drain below the instruments, it was not possible to evaluate the stable atmosphere performance. Good correlations, however, were obtained for carbon dioxide flux.

Consequently, considering only unstable atmospheric cases, regardless of wetness conditions, the results indicate that a site where (1) the EC method provided a moderate imbalance (~10% all data), (2) measurements were taken well

above of a short homogeneous canopy, and (3) regional advection is present late afternoon, SR analysis was reliable for determining sensible heat, latent heat, and carbon dioxide fluxes independently for a long-term evaluation. SR and EC analysis had similar Bowen ratio estimates.

Acknowledgements

The authors gratefully acknowledge Asun, Carla and Tania for their help in using various facilities at the University of Lleida and the review task made by two anonymous referees which comments help us to improve the paper. We thank Mr. Ted Hehn, Liukang Xu and Siyan Ma for assistance in data collection and processing and Mr. and Mrs Fran Vaira for access to their land. This work was supported by the US Dept of Energy (US DOE grant DE-FG02-06ER64308) and the California Agricultural Experiment Station, TRANSCLA and Ministerio de Educación y Ciencia of Spain.

Appendix A. Determination of the ramp dimensions

As the two ramp models provide similar results when determining ramp amplitude (Chen et al., 1997a), structure functions (Eq. (A.1)) and analysis technique (Eqs. (A.2)–(A.4)) from Van Atta (1977) were applied:

$$S^n(r) = \frac{1}{m-j}\sum_{i=1+j}^{m}(T_i + T_{i-j})^n \tag{A.1}$$

where m is the number of data points in the 30-min interval measured at frequency (f) in Hz, n is the power of the function, j is a sample lag between data points corresponding to a time lag ($r = j/f$), and T_i is the ith temperature sample. An estimate of the mean value for A is determined by solving Eq. (A.2) for the real roots:

$$A^3 + pA + q = 0 \tag{A.2}$$

where

$$p = 10S^2(r) - \frac{S^5(r)}{S^3(r)} \tag{A.3}$$

and

$$q = 10S^3(r) \tag{A.4}$$

According to Chen et al. (1997a), the relationship between the inverse ramp frequency (τ) and ramp amplitude is:

$$\frac{A}{\tau^{1/3}} = -\gamma\left(\frac{S^3(r_x)}{r_x}\right)^{1/3} \tag{A.5}$$

where r_x is the time lag r that maximizes $(S^3(r)/r)$ and γ is a parameter that corrects for the difference between $A/\tau^{1/3}$ and the maximum value of $(S^3(r)/r)^{1/3}$. Parameter γ varies by less than 25% with respect to unity, (0.9–1.2), for the range of canopies in Table A1. For bare soil and straw mulch, parameter γ mainly varies between 1 and 1.2; while for Douglas-fir forest it mainly varies between 0.9 and 1.1. Table A1 shows mean values for parameters γ and r_x and suitable measurement frequencies, in Hz, for different canopies required to solve (A.5) (i.e. to find the appropriate solution to (A.5) for the majority of samples) (Chen et al., 1997a,b).

Table A1 – Recommended mean values for γ, r_x (in seconds), and sampling frequencies (in Hz) for different canopies

Canopy and height	γ	Hz	r_x
Fir forest (16.7 m)	1.001	5	0.833
Straw mulch (0.06 m)	1.175	11	0.111
Bare soil	1.104	26	0.066

Appendix B. Determination of the scalar SR fluxes

The procedure used to solve Eq. (6) is valid for measurements taken over homogeneous vegetation at a single level within the inertial sub-layer. According to Brutsaert (1988) and Wieringa (1993), for homogeneous and dense canopies, the zero-plane displacement, d, and the aerodynamic surface roughness length, z_o, can accurately be estimated as a portion of the canopy height, h, as follows, $d = 0.7$ h and $z_o = 0.12$ h. By virtue of the wind profile law, friction velocity can be estimated as follows (Brutsaert, 1988)

$$u_* = \frac{k u_r}{\ln((z_r - d)/z_0) - \Psi_m(\varsigma)} \tag{B.1}$$

where, u_r is the wind speed at reference height z_r, and $\Psi_m(\zeta)$ is the integrated Businger-Dyer relationship for momentum (Paulson, 1970)

$$\Psi_m(\varsigma) = \begin{cases} 2\ln(0.5(1+x)) + \ln(0.5(1+x^2)) & \zeta \le 0 \\ -2\arctan(x) + 0.5\pi & \\ -4.7\zeta & \zeta > 0 \end{cases} \tag{B.2}$$

where $x = (1 - 16\zeta)^{1/4}$.

The stability parameter and the ramp amplitude for temperature have different sign (Fig. 1b). Therefore, after determining the ramp dimensions (Appendix A) for temperature, the appropriate expressions for $\phi_h(\zeta)$, Eq. (9), and $\Psi_m(\zeta)$, (Eq. (B.2)) are known. Next, the sensible heat flux, ζ and u_* can simultaneously be solved by iteration as follows. Initially, to start the iteration procedure, neutral conditions are assumed for the actual atmospheric surface layer to obtain a first approximation for the friction velocity using Eqs. (B.1) and (B.2). This gives an approximation of the actual friction velocity, parameter α and the sensible heat flux, Eqs. (7) and (6), respectively. Next, through L_o, (Eq. (8)), the first approximation for the stability parameter is provided. The process is iterated until convergence is achieved (for instance, when friction velocity after iteration does not changes as much as 0.005 m s^{-1}). The water vapor and carbon dioxide fluxes were determined using as input in Eqs. (6) and (7) the corresponding

ramp dimensions and the stability parameter and friction velocity previously obtained.

REFERENCES

Anderson, F.E., Snyder, R.L., Miller, R., Drexler, J., 2003. A micrometeorological investigation of a restored California wetland ecosystem. Bull. Am. Meteorol. Soc. 84 (9), 1170–1172.

Baldocchi, D.D., 2008. 'Breathing' of the terrestrial biosphere: lessons learned from a global network of carbon dioxide flux measurement systems. Aust. J. Bot. 56, 1–26.

Baldocchi, D.D., 1997. Flux footprints under forest canopies. Bound. Layer Meteorol. 85, 273–292.

Baldocchi, D.D., Liukang, X., Kiang, N., 2004. How plant functional-type, weather, seasonal drought, and soil physical properties alter water and energy fluxes of an oak-grass savanna and an annual grassland. Agric. For. Meteorol. 123, 13–39.

Beyrich, F., Leps, J.P., Mauder, M., Bange, U., Foken, T., Huneke, S., Lohse, H., Lüdi, A., Meijninger, W.M.L., Mironov, D., Weisensee, U., Zittel, P., 2006. Area-averaged surface fluxes over the LITFASS region on eddy-covariance measurements. Bound. Layer Meteorol. 121, 33–65.

Brutsaert, W., 1988. Evaporation into the Atmosphere. D. Reidel P.C, Dordrecht, Holland.

Businger, J.A., 1988. A note on the Businger-Dyer profiles. Bound. Layer Meteorol. 42, 145–151.

Castellvi, F., Perez, P.J., Ibañez, M., 2002. A method based on high frequency temperature measurements to estimate sensible heat flux avoiding the height dependence. Water Resour. Res. 38, W01084, doi:10.1029/2001WR000486.

Castellvi, F., 2004. Combining surface renewal analysis and similarity theory: a new approach for estimating sensible heat flux. Water Resour. Res. 40, W05201, doi:10.1029/2003WR002677.

Castellvi, F., Martinez-Cob, A., 2005. Estimating sensible heat flux using surface renewal analysis and the variance method. A study case over olive trees at Sastago (NE, Spain). Water Resour. Res. 41, W09422, doi:10.1029/2005WR004035.

Castellvi, F., Snyder, R.L., Baldocchi, D.D., Martinez-Cob, A., 2006a. A comparison of new and existing equations for estimating sensible heat flux using surface renewal and similarity concepts. Water Resour. Res. 42, W08406, doi:10.1029/2005WR004642.

Castellvi, F., Martinez-Cob, A., Perez, O., 2006b. Estimating sensible and latent heat fluxes over rice using surface renewal. Agric. For. Meteorol. 139 (1–2), 164–169, doi:10.1016/j.agrformet.2006.07.005.

Chen, W., Novak, M.D., Black, T.A., Lee, X., 1997a. Coherent eddies and temperature structure functions for three contrasting surfaces. Part I: Ramp model with finite micro-front time. Bound. Layer Meteorol. 84, 99–123.

Chen, W., Novak, M.D., Black, T.A., Lee, X., 1997b. Coherent eddies and temperature structure functions for three contrasting surfaces. Part II: Renewal model for sensible heat flux. Bound. Layer Meteorol. 84, 125–147.

De Bruin, H.A.R., Van Den Hurí, B.J.J.M., Kroon, L.J.M., 1999. On the temperature-humidity correlation and similarity. Bound. Layer Meteorol. 93, 453–468.

Drexler, J.Z., Snyder, R.L., Spano, D., Paw U, K.T., 2004. A review of models and micrometeorological methods used to estimate wetland evapotranspiration. Hydrol. Process. 18, 2071–2101.

Dyer, A.J., 1974. A review of flux–profile relationships. Bound. Layer Meteorol. 7, 363–372.

Finnigan, J.J., Clement, R., Malhi, Y., Leuning, R., Cleugh, H.A., 2003. A re-evaluation of long-term flux measurement techniques part I: averaging and coordinate rotation. Bound. Layer Meteorol. 107, 1–48.

Foken, T., Wichura, B., 1996. Tools for quality assessment of surface-based flux measurements. Agric. For. Meteorol. 78, 83–105.

Foken, T., 2006. 50 years of the Monin-Obukhov similarity theory. Bound. Layer Meteorol. 119, 431–447.

Foken, T., Mauder, M., Liebethal, C., Wimmer, F., Beyrich, F., Raasch, S., DeBruin, H.A.R., Meijninger, W.M.L., Bange, J., 2006. Attempt to close the energy balance for the LITFASS-2003 experiment, 27th Symposium on Agricultural and Forest Meteorology. American Meteorological Society, San Diego, paper 1.11.

Fuchs, M., Tanner, C.B., 1967. Evaporation from a drying soil. J. Appl. Meteorol. 6, 852–857.

Gao, W., Shaw, R.H., Paw U, K.T., 1989. Observation of organized structure in turbulent flow within and above a forest canopy. Bound. Layer Meteorol. 47, 349–377.

Higbie, R., 1935. The rate of absorption of a pure gas into a still liquid during short periods of exposure. Trans. Am. Inst. Chem. Eng. 31, 355–388.

Högström, U., 1988. Non-dimensional wind and temperature profiles in the atmospheric surface layer: a re-evaluation. Bound. Layer Meteorol. 42, 55–78.

Hongyan, C., Jiayi, C., Hu, F., Qingcun, Z., 2004. The coherent structure of water vapour transfer in the unstable atmospheric surface layer. Bound. Layer Meteorol. 111, 534–552.

Inagaki, A., Letzel, M.O., Raasch, S., Kanda, M., 2006. Impact of surface heterogeneity on energy balance: a study using LES. J. Meteorol. Soc. Jpn. 84, 187–198.

Kanda, M., Inagaki, A., Letzel, M.O., Raasch, S., Watanabe, T., 2004. LES study of the energy imbalance problem with eddy covariance fluxes. Bound. Layer Meteorol. 110, 381–404.

Katul, G., Hsieh, C., Oren, R., Ellsworth, D., Philips, N., 1996. Latent and sensible heat flux predictions from a uniform pine forest using surface renewal and flux variance methods. Bound. Layer Meteorol. 80, 249–282.

Kohsiek, W., Liebethal, C., Foken, T., Vogt, R., Oncley, S.P., Bernhofer, Ch., DeBruin, H.A.R., 2007. The energy balance experiment EBEX-2000. Part III: behavior and quality of the radiation measurements. Bound. Layer Meteorol. 123, 55–75.

Kristensen, L., Mann, J., Oncley, S.P., Wyngaard, J.C., 1997. How close is close enough when measuring scalar fluxes with displaced sensors? J. Atmos. Ocean Tech. 14, 814–821.

Laubach, J., Teichmann, U., 1999. Surface energy budget variability: a case study over Grass with special regard to minor inhomogeneities in the source area. Theor. Appl. Climatol. 62, 9–24.

Lee, X., Yu, Q., Sun, X., Liu, J., Min, Q., Liu, Y., Zhang, X., 2004. Micrometeorological fluxes under the influence of regional and local advection: a revisit. Agric. For. Meteorol. 122, 111–124.

Lohou, F., Druilhet, A., Campistron, B., Redelsperger, J.L., Said, F., 2000. Numerical study of the impact of coherent structures on vertical transfers in the atmospheric boundary layer. Bound. Layer Meteorol. 97, 361–383.

Mauder, M., Oncley, S.P., Vogt, R., Weidinger, T., Ribeiro, L., Bernhofer, C., Foken, T., Kosiek, W., De Bruin, H.A.R., Liu, H., 2007. The energy balance experiment EBEX-2000. Part II: Intercomparison of eddy-covariance sensors and post-field data processing methods. Bound. Layer Meteorol. 123, 29–54.

Marth, L., 1988. Flux sampling errors for aircraft and towers. J. Atmos. Ocean. Tech. 15, 416–429.

McNaughton, K.G., Laubach, J., 1998. Unsteadiness as a cause of non-equality of eddy diffusivities for heat and vapour at the base of an advective inversion. Bound. Layer Meteorol. 88, 479–504.

Meyers, T.P., Hollinger, S.E., 2004. An assessment of storage terms in the surface energy balance of maize and soybean. Agric. For. Meteorol. 125, 105–115.

Moore, C.J., 1986. Frequency response corrections for eddy covariance systems. Bound. Layer Meteorol. 37, 17–35.

Mortensen, N.G., 1994. Wind measurements for wind energy applications, a review. In: Wind Energy Conversion 1994: Proceedings of the 16th British Wind Energy Association Conference, Stirling, June 15–17. Br. Wind Energy Assoc., London, pp. 353–360.

Oncley, S.P., Foken, T., Vogt, R., Kohsiek, W., DeBruin, H.A.R., Bernhofer, C., Christen, A., Van Gorsen, E., Grantz, D., Feigenwinter, C., Lehner, I., Liebethal, C., Liu, H., Mauder, M., Pitacco, A., Ribeiro, L., Weidinger, T., 2007. The energy balance experiment EBEX-2000. Part I: overview and energy balance. Bound. Layer Meteorol. 123, 1–28.

Paulson, C.A., 1970. The mathematical representation of wind speed and temperature profiles in the unstable atmospheric surface layer. J. Climate Appl. Meteorol. 9, 857–861.

Paw U, K.T., Qiu, J., Su, H.B., Watanabe, T., Brunet, Y., 1995. Surface renewal analysis: a new method to obtain scalar fluxes without velocity data. Agric. For. Meteorol. 74, 119–137.

Paw U, K.T., Baldocchi, D.D., Meyers, T.P., Wilson, K.B., 2000. Correction of eddy-covariance measurements incorporating both advective effects and density fluxes. Bound. Layer Meteorol. 97, 487–511.

Paw U, K.T., Snyder, R.L., Spano, D., Su, H.B., 2005. Surface renewal estimates of scalar exchanges, Micrometeorology in Agricultural Systems, Agronomy Monograph 47, Chapter 20, ASA-CSSA-SSSA Publishers, Madison (WI, USA).

Snyder, R.L., Spano, D., Paw U, K.T., 1996. Surface renewal analysis for sensible and latent heat flux density. Bound. Layer Meteorol. 77, 249–266.

Spano, D., Snyder, R.L., Duce, P., Paw U, K.T., 1997. Surface renewal analysis for sensible heat flux density using structure functions. Agric. For. Meteorol. 86, 259–271.

Spano, D., Snyder, R.L., Duce, P., Paw U, K.T., 2000. Estimating sensible and latent heat flux densities from grapevine canopies using surface renewal. Agric. For. Meteorol. 104, 171–183.

Spano, D., Snyder, R.L., Duce, P., Paw U, K.T., Falk, M., 2002. Surface renewal determination of scalar fluxes over and old-growth forest. Am. Meteorol. Soc., 25th Conference on Agric. For. Meteorol. 104, 171–183.

Steinfeld, G., Letzel, M.O., Raasch, S., Kanda, M., Inagaki, A., 2007. Spatial representativeness of single tower measurements and the imbalance problem with eddy-covariance fluxes: results of a large eddy simulation study. Bound. Layer Meteorol. 123, 77–98.

Thomas, C., Foken, T., 2007. Flux contribution of coherent structures and its implications for the exchange of energy and matter in a tall spruce canopy. Bound. Layer Meteorol. 123, 317–337.

Twine, T.E., Kustas, W.P., Norman, J.M., Cook, D.R., Houser, P.R., Meyers, T. P., Prueger, J.H., Starks, P.J., Wesely, M.L., 2000. Correcting eddy-covariance flux underestimates over a grassland. Agric. For. Meteorol. 20–24 May, Norfolk, Virginia, USA).

Van Atta, C.W., 1977. Effect of coherent structures on structure functions of temperature in the atmospheric boundary layer. Arch. of Mech. 29, 161–171.

Vickers, D., Mahrt, L., 1997. Quality control and flux sampling problems for tower and aircraft data. J. Atmos. Ocean. Tech. 20, 143–151.

Warhaft, Z., 1976. Heat and moisture flux in the stratified boundary layer. Q. J. R. Meteorol. Soc. 102, 703–707.

Webb, E.K., Pearman, G.I., Leuning, R., 1980. Correction of the flux measurements for density effects due to heat and water vapour transfer. Q. J. R. Meteorol. Soc. 106, 85–100.

Wilson, K., Goldstein, A., Falge, E., Aubinet, M., Baldocchi, D.D., Berbigier, P., Bernhofer, C., Ceulemans, R., Dolman, H., Field, C., Grelle, A., Ibrom, A., Law, B.E., Kowalski, A., Meyers, T., Moncrieff, J., Monson, R., Oechel, W., Tenhumen, J., Valentini, R., Verma, S., 2002. Energy balance closure at FLUXNET sites. Agric. For. Meteorol. 113 223–143.

Wieringa, J., 1993. Representative roughness parameters for homogeneous terrain. Bound. Layer Meteorol. 63, 323–363.

Xu, L., Baldocchi, D.D., 2004. Seasonal variation in carbon dioxide exchange over a Mediterranean annual grassland in California. Agric. For. Meteorol. 123, 79–96.

Zapata, N., Martinez-Cob, A., 2001. Estimation of sensible and latent heat flux from natural sparse vegetation surfaces using surface renewal. J. Hydrol. 254, 215–228.